Stabilized Radiation Pressure Acceleration and Neutron Generation in Ultra-thin Deuterated Foils

A. Alejo,[1,2] H. Ahmed,[1,3] A.G. Krygier,[4] R. Clarke,[3] R.R. Freeman,[4] J. Fuchs,[5] A. Green,[1] J.S. Green,[3] D. Jung,[1] A. Kleinschmidt,[6] J.T. Morrison,[7] Z. Najmudin,[8] H. Nakamura,[8] P. Norreys,[3,9] M. Notley,[3] M. Oliver,[9] M. Roth,[6] L. Vassura,[5] M. Zepf,[1] M. Borghesi,[1] and S. Kar[1,*]

[1]*Centre for Plasma Physics, School of Mathematics and Physics, Queen's University Belfast, BT7 1NN, UK*
[2]*Instituto Galego de Física de Altas Enerxías, Universidade de Santiago de Compostela, Santiago de Compostela 15782, Spain*
[3]*Central Laser Facility, Rutherford Appleton Laboratory, Didcot, Oxfordshire, OX11 0QX, UK*
[4]*Department of Physics, The Ohio State University, Columbus, Ohio 43210, USA*
[5]*LULI, Ecole Polytechnique, CNRS, Route de Saclay, 91128 Palaiseau Cedex,France*
[6]*Institut für Kernphysik, TU Darmstadt, D-64289 Darmstadt, Germany*
[7]*Propulsion Systems Directorate, Air Force Research Lab, Wright Patterson Air Force Base, Ohio 45433, USA*
[8]*Blackett Laboratory, Department of Physics, Imperial College, London SW7 2AZ, UK*
[9]*Department of Physics, University of Oxford, Oxford, OX1 3PU, UK*

(Dated: April 27, 2022)

Premature relativistic transparency of ultrathin, laser-irradiated targets is recognized as an obstacle to achieving a stable Radiation Pressure Acceleration in the 'Light Sail' (LS) mode. Experimental data, corroborated by 2D PIC simulations, show that a few-nm thick overcoat surface layer of high Z material significantly improves ion bunching at high energies during the acceleration. This is diagnosed by simultaneous ion and neutron spectroscopy following irradiation of deuterated plastic targets. In particular, copious and directional neutron production (significantly larger than for other in-target schemes) arises, under optimal parameters, as a signature of plasma layer integrity during the acceleration.

The progress in laser technologies over the past couple of decades has led to an increasing interest in laser-driven ion acceleration and the related development of secondary sources, such as neutrons [1]. Although Target-Normal Sheath Acceleration (TNSA) [1] has been the most studied ion acceleration mechanism, significant attention is given to other promising mechanisms, such as Radiation Pressure Acceleration (RPA) [2–9], which, in principle, has the potential to be extremely efficient with laser intensities beyond 10^{21} W cm^{-2}. Of particular interest is the Light Sail (LS) regime of RPA, in which the laser propels forward the irradiated portion of an ultra-thin target, leading to efficient acceleration of ions in a narrow spectral bandwidth and divergence cone. Experimental data [7] and particle-in-cell (PIC) simulations [2–5] indicate a fast ion energy scaling ($E_{ion} \propto \left[a_0^2\tau_p/\chi\right]^2$, where $a_0^2\tau_p$ and χ represent incident laser fluence on the target and target areal density, respectively) in this regime, which extrapolates to ion energies beyond 100s of MeV/nucleon for upcoming laser facilities [10].

A key requirement for efficient LS acceleration is to maintain the integrity of the ultra-thin target over the duration of the laser pulse. Circular polarisation for ultra-short (10s of fs) laser pulses has been shown to be effective in achieving high ion energies in narrow energy bunches [9], with heavier species supporting the stable acceleration of lighter ions [11]. For longer pulses (in the ps regime), no such significant dependence on polarization has been reported in experiments, which have highlighted instead a hybrid TNSA-RPA regime [7], with an enhancement in proton energy associated to the onset of relativistically induced transparency (RIT) near the peak of the pulse [12].

In this paper, a possible route to avoid premature termination of LS acceleration from ultra-thin foils is investigated experimentally by simultaneous ion and neutron spectroscopy while using foils of deuterated plastic (CD). While CD targets below 300 nm thickness showed a clear signature of the onset of RIT, for the semi-transparent 100 nm thick targets bunched deuterium acceleration was reinforced by adding the high-Z surface layer, a concept which was recently studied using PIC simulations by Shen *et al.* [13]. Stabilisation of the LS acceleration is demonstrated not only by the narrow-band ion spectra, but also by an abrupt (order of magnitude) increase in fast neutrons from the deuterium plasma layer. Highly beamed fast neutrons at fluxes (exceeding 10^9 n/sr above 2.5 MeV) competitive with other approaches [14–19] were produced from the ultra-thin (100*s* of nm) CD foils at optimum conditions. The neutron flux recorded exceeds by more than an order of magnitude the isotropic flux measured from thicker CD targets under similar interaction conditions. Particle-in-cell simulations studying ion acceleration and fast neutron generation endorsed the enhanced ion bunch formation in presence of a sacrificial high-Z species, which maintains the ion layer opaque during the pulse by continuously replenishing it with copious amount of electrons via successive ionisation as the laser intensity ramps up.

The experiment was carried out at the Rutherford

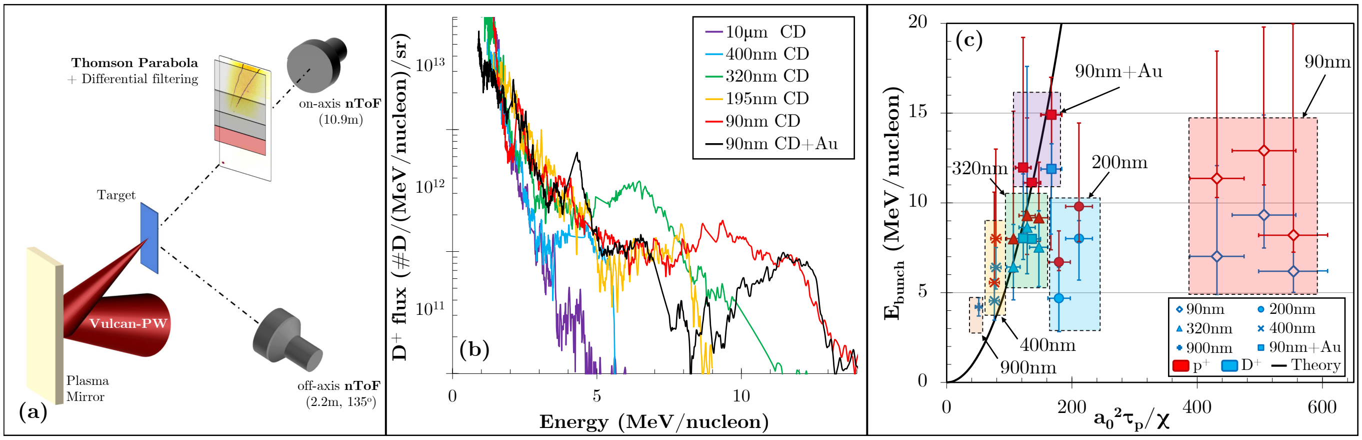

FIG. 1. **(a)** Schematic of the experimental setup. **(b)** On-axis deuteron spectra obtained from a target thickness scan (shots taken with different target thickness, as labelled in the legend) under similar laser conditions ($E_L = (160 \pm 20)$ J, $I_0 = (2.1 \pm 0.3) \times 10^{20}$ W cm^{-2}. **(c)** Proton and deuteron energies at their spectral peaks obtained for different target thicknesses, plotted against the LS scaling parameter, $\Pi \equiv a_0^2 \tau_p/\chi$. The error bars along the y (energy) axis depict the extent of the spectral bunch. The solid line represents the predicted ion energy by the LS-scaling reported in [7].

Appleton Laboratory (RAL), STFC, UK by employing the petawatt arm of the VULCAN laser of wavelength $\lambda_0 = 1053$ nm, pulse duration of 850 ± 150 fs and a repetition rate of 30 minutes [20]. A schematic of the experimental setup is shown in Fig. 1(a). After being reflected off a plasma mirror, the P-polarised laser pulse was focussed down by a $f/3$ parabola to a ~ 5 µm spot onto the target at normal incidence. The range of laser energy (E_L) delivered on target for the data shown in this paper was $100 - 250$ J, corresponding to peak intensity on target (I_0) in the range $(1 - 3) \times 10^{20}$ W cm^{-2}. The targets were made of deuterated plastic ($(C_2D_4)_n$, referred here as CD) with thickness $l = 90 - 900$ nm and 10 µm. The ions accelerated from the targets were diagnosed using Thomson Parabola Spectrometers (TPS). The image plate detector of the TPS was differentially filtered [21] to discriminate deuterium ions across the entire energy range from species with similar charge-to-mass ratios, such as C^{6+} or O^{8+}. Neutrons generated from the laser-irradiated target were diagnosed, along the laser axis and at ~ 135 deg off the laser axis, by using fast plastic scintillator (EJ232Q) detectors in time-of-flight (nToF) configuration. The on- and off-axis nToF detectors were placed at the farthest possible distances (10.9 m and 2.2 m, respectively) from the target, allowed by the target area constraints. Where the energy of the neutrons was obtained from their time-of-flight, the neutron flux was obtained by cross-calibrating the detectors with absolutely calibrated Bubble Detector Spectrometers (BDS), as discussed in Ref. [22].

As expected from the TNSA mechanism, quasi-exponential deuteron spectra with a nominal $\sim$ 5 MeV/nucleon cut-off energy were obtained from the irradiation of thick (10 µm) CD targets, as shown in Fig. 1(b). As the target thickness was gradually reduced down to a few hundreds of nanometres, narrow-bandwidth spectral features, hereafter referred as 'spectral humps', started to appear close to the spectral cut-off alongwith a significant increase in the cut-off energy, as it can be seen from the spectra shown in Fig. 1(b) for 400 nm and 320 nm thick CD targets. Such spectral behaviour for heavy ions (for instance, carbon ions) from ultra-thin targets has been previously reported [7, 9] at the onset of RPA-LS dominance in a TNSA-RPA hybrid regime. In this case, observing spectral modulations for an ion species unique to the target bulk (i.e. deuterium) corroborates further our understanding of the RPA-LS mechanism in ultrathin targets.

In addition to the spectra shown in Fig. 1(b), further ion spectra were obtained over a number of shots by varying the target thickness in the range 900 nm to 90 nm. For target thickness down to 320 nm, the spectral humps in proton and deuteron spectra were found to be in good agreement with the RPA-LS scaling [7], as shown in Fig. 1(c). The energies at the spectral humps for the deuterons were slightly lower than those for the protons, as expected in a multi-species scenario [7]. The expected rate of increase in ion energy while reducing the target thickness ($E_{ion} \propto \chi^{-2}$), however, did not continue below 320 nm. As it can be seen in Fig. 1(b), 200 nm and 90 nm targets showed significantly broad ended spectral humps, and as shown in Fig. 1(c), at energies significantly below those expected for a stable RPA-LS acceleration. Such behaviour is an indication of targets undergoing RIT part way through the laser pulse [7, 8]. In fact, significantly high laser transmission through such low areal mass density targets has been recently reported [12] under very similar interaction conditions. As discussed later, RIT could be avoided by adding a few nm thick coating of a high-Z material to the ultrathin targets, as observed for the *90nm CD + Au* target shown in Fig. 1(b).

Using targets of deuterated plastic allowed us to study

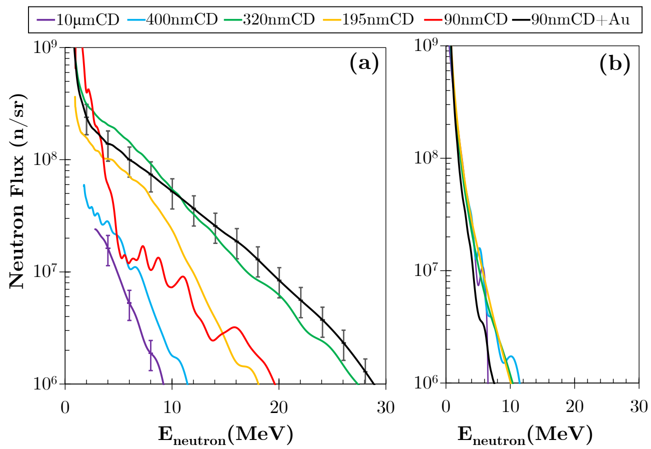

FIG. 2. Neutron spectra measured simultaneously to the results in Fig. 1(b), along **(a)** the laser axis, and **(b)** 135 deg off the laser axis respectively. The error bars, only plotted over two representative cases in (a) for clarity, represent the uncertainty in measuring neutron spectra by the ToF detectors in the current setup.

neutron generation from the ultrathin foils, which in turn provides information about the ion evolution during the interaction. A comparison between the on- and off-axis neutron spectra, obtained from the same set of shots plotted in Fig. 1(b), is shown in Fig. 2(a) and Fig. 2(b), respectively. As one can see, a fairly isotropic, low flux ($(5.9 \pm 1.8) \times 10^7$ n/sr for energy above 2.5 MeV) neutron emission was produced from 10 μm thick CD foils, similar to that reported in Ref. [23]. The neutrons in this case are most likely produced at the target front surface, either from the thermonuclear reactions in the hot dense plasma produced by the laser interaction, or by the ions produced by the hole-boring mechanism driven into the target bulk [23, 24]. Reducing target thickness, one would expect either a minimal or an adverse effect on the neutron yield as produced via these mechanisms. On the contrary, sub-micron thick targets (for instance the 320 nm target shown in Fig. 1(b)) produced a dramatic increase in the neutron flux ($(1.3 \pm 0.4) \times 10^9$ n/sr for neutron energy above 2.5 MeV) in a beam that is highly peaked (ratio between on- and off- axis fluxes ~ 11) along the laser forward direction.

An abrupt increase in neutron flux, together with a beamed feature is consistent for the case where a dense plasma 'sail' is driven by the radiation pressure of the laser for a sufficiently long duration, as can be seen in Fig. 3. A pronounced spectral hump, as shown for the 320 nm target in Fig. 1(b) for instance, represents a dense bunch of deuterium ions moving along the laser forward direction with a narrow velocity spread, which was modelled in 3D using the VSIM code [25, 26], enabling binary reactions between the deuterium macro-particles. The simulation was setup with grid size of 0.1 μm in each direction and a $10 \times 10 \times 0.2\,\mu\text{m}^3$ '*sail*' of deuterium ions loaded to the simulation with 50 macro-particles-per-cell and with a given spectral distribution (spectral peaks and FWHM bandwidths are mentioned in the respective figures). While the d-d reactions inside the *sail* produce neutrons isotropically in its centre-of-mass frame (as it can be seen in Fig. 3(b) for a quasi-stationary bunch), neutron emission from a moving *sail* will appear highly anisotropic in the lab frame, depending on its centre-of-mass (CoM) velocity, as it can be seen in Fig. 3(a) and (b). While the forward-moving neutrons gain energy in the lab-frame, the neutrons emitted backwards in the CoM frame are either moderated or forced to reverse their direction depending on the CoM velocity, effectively doubling the neutron flux in the forward direction. The maximum neutron energy (E_n) along the ion beam axis can be derived similarly to Ref. [23] considering energy-momentum conservation [27] and is given by $E_n = (E_d/4)(\sqrt{2} + \sqrt{3\mathcal{Q}/E_d})^2$, in terms of the average kinetic energy of the deuterium ions (E_d) in the *sail* and the Q-value of the reaction ($\mathcal{Q}$). As shown in Fig. 3(c), the energies of the neutrons and deuterons produced in each shot with sub-micron CD targets shown in Fig. 1(c), shows a very good agreement with the tunability expected from the reaction kinematics in a moving *sail*, which is also reproduced by the VSIM simulations carried out for deuterium *sails* of different energies, with neutrons' angular distribution as shown in Fig. 3(b). The ability to tune the energy of fast neutrons provides an unique perspective for pre-moderation down to sub-MeV range for an efficient conversion to epithermal and thermal energies [28, 29].

A unique insight into the LS phase of acceleration and its connection to the onset of RIT is gained by considering together the neutron emission and the ion spectra in the experimental data. For example, the neutron flux for 90 nm CD targets was an order of magnitude lower compared to the case of 320 nm CD targets, whereas the former produced deuterium spectra with higher energy and comparable flux compared to the latter. Based on the model simulations shown in Fig. 3(d), such scenario can be explained on the basis of a significantly broader spectral profile for deuterons obtained in the former case, suggesting 90 nm thick target undergoes RIT during the laser interaction. For ultra-thin targets, RPA has been shown to be very sensitive to target decompression via electron heating as well as transverse instabilities [9, 30]. Direct interaction of intense laser with a semi-transparent plasma has been shown to lead to some enhancement in ion energies [12], however with a broad spectral profile unlike the one expected from LS acceleration alone. Indeed, targets thinner than 320 nm, as shown in the Fig. 1(c), have produced ion energies significantly lower than expected from acceleration in a LS-dominated regime.

As mentioned earlier, an effective way to overcome target transparency is by providing the target a surplus of electrons, for instance by using a thin coating of high-Z

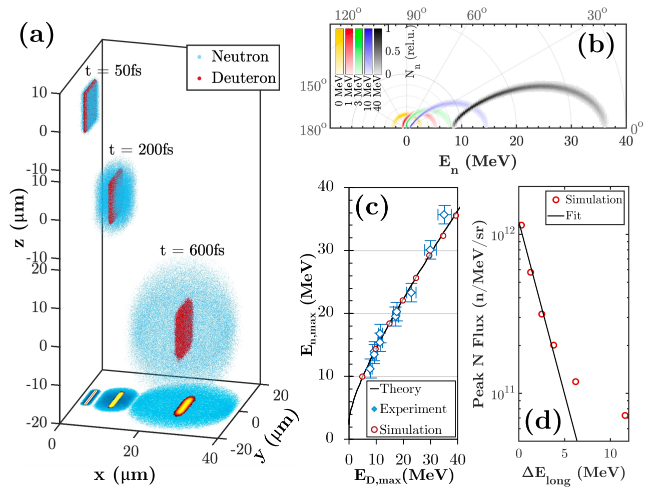

FIG. 3. **(a)** 3D and 2D-projection plots showing neutron (blue) production at different times (as labelled above) from a dense '*sail*' of deuterium ions (red) moving along the X-axis with a spectral distribution peaked at 20 MeV and FWHM width of 1 MeV, obtained from VSIM simulations. **(b)** Angular distribution of neutrons produced from *sails* of deuterium ions of narrow spectral distribution of 1 MeV FWHM, peaked at different energies as shown in the figure. The color bar represent neutron flux normalised for each case. **(c)** Deuteron vs. neutron energies obtained in different shots shown in Fig 1(c), compared with the energies expected from reaction kinematic (analytical) and VSIM simulations for *sails* of dense bunch of deuterium ions. **(d)** Peak neutron flux along the X-axis (emitted within a small cone of 5 degrees) from *sails* of deuterium ions of spectral distribution peaked at 20 MeV and varying the spectral width (ΔE_{long}).

material on the target [13]. Although the overall target areal density is doubled by adding a thin Au layer of 5 nm, the '*90nm CD+Au*' target produced deuteron spectra with a pronounced spectral hump at higher energy (as shown in Fig. 1(b)), agreeing well with the RPA-LS scaling shown in Fig. 1(c). Furthermore, the on-axis neutron flux from the *90nm CD+Au* target ($(1.1\pm0.4)\times10^9$ n/sr) for neutron energy above 2.5 MeV) was an order of magnitude higher than the 90 nm CD target, even though the deuteron flux and cut-off energies from both targets were similar. Therefore, it is the narrow-band spectral bunch that led to the abrupt increase in neutron yield in case of the *90nm CD+Au*, as supported by the VSIM simulations shown in Fig. 3(d). This indicates that the loss of efficiency of RPA-LS as acceleration mechanism below 320 nm is being remedied by adding a sacrificial high-Z layer.

2D PIC simulations were performed using the EPOCH code [31] in order to corroborate further the experimental results obtained for the three cases - 320nm CD, 90nm CD and *90nm CD+Au*. Due to the computational limitation for ps-scale simulations, the setup parameters were scaled down while maintaining $I_0/\rho c^3$ and $a_0^2\tau_p/\chi$ constant, as carried out in Ref. [7]. The laser pulse was modelled as p-polarised, λ=1.053 µm, 300 fs FWHM duration, Gaussian spot of 5 µm radius with peak intensity $I_0 = 3.0\times10^{19}$ W cm^{-2}. The CD target (99% CD, 1% CH) was modelled with density $\rho_{\rm CD}$ =0.21 g cm^{-3}. The scaled down thicknesses for the 90 nm and 320 nm targets in the experiment were calculated as 36 nm and 128 nm, respectively. The 5nm thick Au layer was modelled as a 2 nm Au layer of density ρ_{Au}=4.13 g cm^{-3} at the rear side of the CD target. All the species were initialised as neutral atoms, with ionisation state dynamically calculated considering their atomic potentials [32]. Finally, 3 nm thick CH layers were added on both sides of the target to simulate contaminant layers.

As shown in Fig. 4(a,1), the 320 nm CD target remains reflective at the peak of the laser pulse, allowing for an effective LS acceleration. Looking at the off laser axis in Fig. 4(a,3), as marked by the black markers, one can see a clear detachment of the dense deuterium sail from the bulk plasma, suggesting an efficient LS-RPA mechanism at work. On the other hand, the 90 nm CD target becomes fully transparent (see Fig. 4(b,1)), before the laser intensity on the target reaches its peak value producing a quasi-uniform ion distribution with a marginal density pile-up at the leading edge (as shown inFig. 4(b,4)), typical of a blow-out interaction regime. For the *90nm CD+Au* case, the presence of the high-Z layer maintained the target opacity during the laser pulse. While a linearly polarised laser pulse cause strong electron heating, leading rapidly to a transparency regime (as in case of 90 nm CD - Fig. 4(b)), the simulation shows that the Au ions replenish electrons to the interaction region in a highly

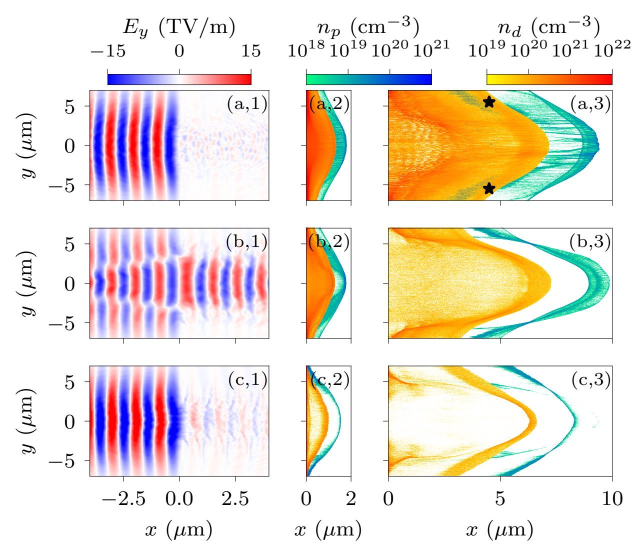

FIG. 4. Laser electric field **(*,1)**, proton (n_p) and deuterium ion (n_d) number density as the peak intensity reaches the target **(*,2)** and at the end of the simulation ($\sim$ 200 fs after the peak intensity) **(*,3)**, obtained by PIC simulations, for three different thickness of the target: 320nm **(a,*)**, 90nm **(b,*)** and 90nm CD+Au **(c,*)**. Colorbars for proton and deuteron densities are common to (*,2) and (*,3).

self-organised fashion due to the dynamic ionisation. As shown in Fig. 4(c,3), the deuterium ions remain highly bunched until relatively long after the laser pulse, which is a clear indication of achieving a stable RPA-LS acceleration. Such a dense and lasting bunch of ions is the source of increased neutron flux observed in the experiment.

Simultaneous ion and neutron spectroscopy offered a unique way of gaining insight into the laser-target interaction dynamics, which is extremely difficult otherwise to measure by conventional diagnostics. The scheme of using high-Z flash coating allowed to extend LS to thinner targets (and higher bunched energies), which was experimentally demonstrated in this paper. Highly beamed fast neutrons exceeding 10^9 n/sr above 2.5 MeV were measured from the ultra-thin (100*s* of nm) CD foils without using secondary converters, which in turn shows a novel route to an intense and tunable neutron source competitive with other approaches [14–19], with an intrinsic ultra-short (10s of ps) burst duration. Since the neutron yield depends directly on the square of ion density and fusion burn time, there is significant scope for optimising the brightness of the LS-driven neutron source by tuning laser and target parameters. Furthermore, the LS-driven neutron source also provides the unique perspective of pre-moderating neutrons down to the sub-MeV range for an efficient conversion to epithermal and thermal sources.

The authors acknowledge funding from EPSRC [EP/J002550/1-Career Acceleration Fellowship held by S. K., EP/L002221/1, EP/E035728/1, EP/K022415/1, EP/J500094/1 and EP/I029206/1]. AA and SK acknowledge useful discussions with Dr. A.P.L. Robinson from STFC, UK. Authors also acknowledge the support of the target fabrication and mechanical engineering staff of the Central Laser Facility, STFC, UK. Computing resources provided by STFC Scientific Computing Department's SCARF cluster.

---

* s.kar@qub.ac.uk

[1] A. Macchi, M. Borghesi, and M. Passoni, Reviews of Modern Physics **85**, 751 (2013).

[2] T. Esirkepov, M. Borghesi, S. Bulanov, G. Mourou, and T. Tajima, Highly efficient relativistic-ion generation in the laser-piston regime, Physical Review Letters **92**, 175003 (2004).

[3] A. Robinson, M. Zepf, S. Kar, R. Evans, and C. Bellei, Radiation pressure acceleration of thin foils with circularly polarized laser pulses, New Journal of Physics **10**, 013021 (2008).

[4] B. Qiao, S. Kar, M. Geissler, P. Gibbon, M. Zepf, and M. Borghesi, Dominance of radiation pressure in ion acceleration with linearly polarized pulses at intensities of 10^{21} w cm^{-2}, Physical Review Letters **108**, 115002 (2012).

[5] B. Qiao, M. Zepf, M. Borghesi, and M. Geissler, Stable gev ion-beam acceleration from thin foils by circularly polarized laser pulses, Physical review letters **102**, 145002 (2009).

[6] S. Kar, M. Borghesi, S. Bulanov, M. Key, T. Liseykina, A. Macchi, A. Mackinnon, P. Patel, L. Romagnani, A. Schiavi, *et al.*, Plasma jets driven by ultraintense-laser interaction with thin foils, Physical Review Letters **100**, 225004 (2008).

[7] S. Kar, K. Kakolee, B. Qiao, A. Macchi, M. Cerchez, D. Doria, M. Geissler, P. McKenna, D. Neely, J. Osterholz, *et al.*, Ion acceleration in multispecies targets driven by intense laser radiation pressure, Physical Review Letters **109**, 185006 (2012).

[8] A. Macchi, S. Veghini, T. V. Liseykina, and F. Pegoraro, Radiation pressure acceleration of ultrathin foils, New Journal of Physics **12**, 045013 (2010).

[9] C. Scullion, D. Doria, L. Romagnani, A. Sgattoni, K. Naughton, D. Symes, P. McKenna, A. Macchi, M. Zepf, S. Kar, *et al.*, Polarization dependence of bulk ion acceleration from ultrathin foils irradiated by high-intensity ultrashort laser pulses, Physical Review Letters **119**, 054801 (2017).

[10] Extreme light infraestracture (eli), `http://www.eli-np.ro//` (2020).

[11] S. Steinke, P. Hilz, M. Schnürer, G. Priebe, J. Bränzel, F. Abicht, D. Kiefer, C. Kreuzer, T. Ostermayr, J. Schreiber, *et al.*, Stable laser-ion acceleration in the light sail regime, Physical Review Special Topics-Accelerators and Beams **16**, 011303 (2013).

[12] A. Higginson, R. Gray, M. King, R. Dance, S. Williamson, N. Butler, R. Wilson, R. Capdessus, C. Armstrong, J. Green, S. Mirfayzi, *et al.*, Near-100 mev protons via a laser-driven transparency-enhanced hybrid acceleration scheme, Nature Communications **9**, 724 (2018).

[13] X. Shen, B. Qiao, H. Zhang, S. Kar, C. Zhou, H. Chang, M. Borghesi, and X. He, Achieving stable radiation pressure acceleration of heavy ions via successive electron replenishment from ionization of a high-z material coating, Physical Review Letters **118**, 204802 (2017).

[14] D. Higginson, J. McNaney, D. Swift, G. Petrov, J. Davis, J. Frenje, L. Jarrott, R. Kodama, K. Lancaster, A. Mackinnon, *et al.*, Production of neutrons up to 18 mev in high-intensity, short-pulse laser matter interactions, Physics of Plasmas **18**, 100703 (2011).

[15] M. Roth, D. Jung, K. Falk, N. Guler, O. Deppert, M. Devlin, A. Favalli, J. Fernandez, D. Gautier, M. Geissel, R. Haight, C. E. Hamilton, B. M. Hegelich, R. P. Johnson, F. Merrill, G. Schaumann, K. Schoenberg, M. Schollmeier, T. Shimada, T. Taddeucci, J. L. Tybo, F. Wagner, S. A. Wender, C. H. Wilde, and G. A. Wurden, Bright laser-driven neutron source based on the relativistic transparency of solids, Phys. Rev. Lett. **110**, 044802 (2013).

[16] A. Kleinschmidt, V. Bagnoud, O. Deppert, A. Favalli, S. Frydrych, J. Hornung, D. Jahn, G. Schaumann, A. Tebartz, F. Wagner, G. Wurden, B. Zielbauer, and M. Roth, Intense, directed neutron beams from a laser-driven neutron source at phelix, Physics of Plasmas **25**, 053101 (2018), https://doi.org/10.1063/1.5006613.

[17] K. Lancaster, S. Karsch, H. Habara, F. Beg, E. Clark, R. Freeman, M. Key, J. King, R. Kodama, K. Krushelnick, *et al.*, Characterization of 7 li (p, n) 7 be neutron

yields from laser produced ion beams for fast neutron radiography, Physics of plasmas **11**, 3404 (2004).

[18] C. Zulick, F. Dollar, V. Chvykov, J. Davis, G. Kalinchenko, A. Maksimchuk, G. Petrov, A. Raymond, A. Thomas, L. Willingale, *et al.*, Energetic neutron beams generated from femtosecond laser plasma interactions, Applied Physics Letters **102**, 124101 (2013).

[19] G. M. Petrov, D. P. Higginson, J. Davis, T. B. Petrova, J. M. Mcnaney, and C. Mcguffey, Generation of high-energy ($>$ 15 MeV) neutrons using short pulse high intensity lasers Generation of high-energy ($>$ 15 MeV) neutrons using short pulse high intensity lasers, Physics of Plasmas **19**, 093106 (2012).

[20] C. Danson, P. Brummitt, R. Clarke, J. Collier, B. Fell, A. Frackiewicz, S. Hancock, S. Hawkes, C. Hernandez-Gomez, P. Holligan, *et al.*, Vulcan petawattan ultra-high-intensity interaction facility, Nuclear Fusion **44**, S239 (2004).

[21] A. Alejo, S. Kar, H. Ahmed, A. Krygier, D. Doria, R. Clarke, J. Fernandez, R. Freeman, J. Fuchs, A. Green, J. Green, D. Jung, A. Kleinschmidt, C. Lewis, J. Morrison, Z. Najmudin, H. Nakamura, G. Nersisyan, P. Norreys, M. Notley, M. Oliver, M. Roth, J. Ruiz, L. Vassura, M. Zepf, and M. Borghesi, Characterisation of deuterium spectra from laser driven multi-species sources by employing differentially filtered image plate detectors in thomson spectrometers, Review of Scientific Instruments **85**, 10.1063/1.4893780 (2014).

[22] S. Mirfayzi, S. Kar, H. Ahmed, A. Krygier, A. Green, A. Alejo, R. Clarke, J. Fernandez, R. Freeman, J. Fuchs, J. Green, D. Jung, A. Kleinschmidt, C. Lewis, J. Morrison, Z. Najmudin, H. Nakamura, G. Nersisyan, P. Norreys, M. Notley, M. Oliver, M. Roth, J. Ruiz, L. Vassura, M. Zepf, and M. Borghesi, Calibration of time of flight detectors using laser-driven neutron source, Review of Scientific Instruments **86** (2015).

[23] S. Kar, A. Green, H. Ahmed, A. Alejo, A. Robinson, M. Cerchez, R. Clarke, D. Doria, S. Dorkings, J. Fernandez, *et al.*, Beamed neutron emission driven by laser accelerated light ions, New Journal of Physics **18**, 053002 (2016).

[24] P. Norreys, A. Fews, F. Beg, A. Bell, A. Dangor, P. Lee, M. Nelson, H. Schmidt, M. Tatarakis, and M. Cable, Neutron production from picosecond laser irradiation of deuterated targets at intensities of, Plasma physics and controlled fusion **40**, 175 (1998).

[25] C. Nieter and J. R. Cary, Vorpal: a versatile plasma simulation code, Journal of Computational Physics **196**, 448 (2004).

[26] VSIM, `www.txcorp.com` for information on electromagnetic and electrostatic simulation with VSim software. (2020).

[27] N. Izumi, Y. Sentoku, H. Habara, K. Takahashi, F. Ohtani, T. Sonomoto, R. Kodama, T. Norimatsu, H. Fujita, Y. Kitagawa, *et al.*, Observation of neutron spectrum produced by fast deuterons via ultraintense laser plasma interactions, Physical Review E **65**, 036413 (2002).

[28] S. Mirfayzi, A. Alejo, H. Ahmed, D. Raspino, S. Ansell, L. Wilson, C. Armstrong, N. Butler, R. Clarke, A. Higginson, *et al.*, Experimental demonstration of a compact epithermal neutron source based on a high power laser, Applied Physics Letters **111**, 044101 (2017).

[29] S. Mirfayzi, H. Ahmed, D. Doria, A. Alejo, S. Ansell, R. Clarke, B. Gonzalez-Izquierdo, P. Hadjisolomou, R. Heathcote, T. Hodge, *et al.*, A miniature thermal neutron source using high power lasers, Applied Physics Letters **116**, 174102 (2020).

[30] A. Sgattoni, S. Sinigardi, L. Fedeli, F. Pegoraro, and A. Macchi, Laser-driven rayleigh-taylor instability: plasmonic effects and three-dimensional structures, Physical Review E **91**, 013106 (2015).

[31] T. Arber, K. Bennett, C. Brady, A. Lawrence-Douglas, M. Ramsay, N. Sircombe, P. Gillies, R. Evans, H. Schmitz, A. Bell, *et al.*, Contemporary particle-in-cell approach to laser-plasma modelling, Plasma Physics and Controlled Fusion **57**, 113001 (2015).

[32] D. R. Lide, *CRC handbook of chemistry and physics* (CRC press, 2004).